UCRL-9222

UNIVERSITY OF CALIFORNIA

Ernest O. Lawrence Radiation Laboratory

TWO-WEEK LOAN COPY

This is a Library Circulating Copy which may be borrowed for two weeks. For a personal retention copy, call Tech. Info. Division, Ext. 5545

BERKELEY, CALIFORNIA

DISCLAIMER

This document was prepared as an account of work sponsored by the United States Government. While this document is believed to contain correct information, neither the United States Government nor any agency thereof, nor the Regents of the University of California, nor any of their employees, makes any warranty, express or implied, or assumes any legal responsibility for the accuracy, completeness, or usefulness of any information, apparatus, product, or process disclosed, or represents that its use would not infringe privately owned rights. Reference herein to any specific commercial product, process, or service by its trade name, trademark, manufacturer, or otherwise, does not necessarily constitute or imply its endorsement, recommendation, or favoring by the United States Government or any agency thereof, or the Regents of the University of California. The views and opinions of authors expressed herein do not necessarily state or reflect those of the United States Government or any agency thereof or the Regents of the University of California.

For Publication in Physical Review

UCRL-9222

UNIVERSITY OF CALIFORNIA
Lawrence Radiation Laboratory
Berkeley, California

Contract No. W. 7405-eng-48

CHARGE-EXCHANGE SCATTERING OF NEGATIVE PIONS BY HYDROGEN AT 230, 260, 290, 317 and 371 MEV

John C. Caris, Robert W. Kenney,
Victor Perez-Mendez, and Walton A. Perkins, III

June 8, 1960

CHARGE-EXCHANGE SCATTERING OF NEGATIVE PIONS BY HYDROGEN AT 230, 260, 290, 317 and 371 MEV

John C. Caris, Robert W. Kenney,
Victor Perez-Mendez, and Walton A. Perkins, III

Lawrence Radiation Laboratory
University of California
Berkeley, California

June 8, 1960

ABSTRACT

The differential cross section for charge-exchange scattering of negative pions by hydrogen has been observed at 230, 260, 290, 317, and 371 Mev. The reaction was observed by detecting one gamma ray from the π^0 decay with a scintillation-counter telescope. A least-squares analysis was performed to fit the observations to the function*

$$\frac{d\sigma}{d\omega} = \sum_{\ell=1}^{5} a_\ell P_{\ell-1} (\cos \theta)$$

in the c.m. frame. The best fit to our experimental measurements requires only s- and p-wave scattering. The results (in mb) are:

	a_1	a_2	a_3
230 ± 9 Mev	2.50 ± 0.10	1.39 ± 0.15	2.73 ± 0.28
260 ± 7	2.02 ± 0.08	1.75 ± 0.14	2.15 ± 0.22
290 ± 9	1.45 ± 0.06	1.80 ± 0.10	1.89 ± 0.18
317 ± 8	1.40 ± 0.06	1.85 ± 0.10	1.50 ± 0.17
371 ± 9	1.08 ± 0.05	1.63 ± 0.08	1.18 ± 0.12

The least-squares analysis indicates that d-wave scattering is not established in this energy range.

*See (4) et seq.

CHARGE-EXCHANGE SCATTERING OF NEGATIVE PIONS BY HYDROGEN AT 230, 260, 290, 317 and 371 Mev*

John C. Caris, Robert W. Kenney,
Victor Perez-Mendez, and Walton A. Perkins, III †

Lawrence Radiation Laboratory
University of California
Berkeley, California

June 8, 1960

I. INTRODUCTION

The purpose of this experiment was to investigate the differential scattering cross section for the reaction

$$\pi^- + p \rightarrow \pi^0 + n \rightarrow 2\gamma + n \qquad (1)$$

in the energy range from 230 to 370 Mev, paying special attention to the search for d-wave scattering.

We note that evidence for d-wave scattering has recently been established within this energy range for π^+-proton[1] and π^--proton[2] elastic scattering.

The results of our work are: a significant reduction in the experimental errors in the angular distribution coefficients previously reported within this energy range,[3,4] and that we have found no evidence for a d-wave contribution to charge-exchange scattering within this energy range. Statistical goodness-of-fit criteria indicate that s- and p-wave scattering adequately fit the measurements.

---

*Research was performed under the auspices of the U.S. Atomic Energy Commission.

†Now at Lawrence Radiation Laboratory, Livermore, California

The charge-exchange reaction cannot be observed directly, since the π^0 meson decays isotropically in its own rest frame in a time somewhat less than 10^{-16} sec. One must deduce the π^0 angular distribution from a gamma-ray distribution observed in the laboratory system. The laboratory-system photon distribution is aberrated in direction and Doppler-shifted in frequency by the motion of the π^0 meson.

The effort to detect d-wave scattering included the extension of the range of angular-distribution measurements and an improvement in the counter-telescope calibration.

First, we were able to measure the photon flux at 0 deg (lab), where d-waves would have a significant effect on the distribution's shape. We knew of no charge-exchange data forward of 15 deg (lab).

Secondly, the absolute efficiency of the photon counter as a function of incident photon energy was measured and was included in the analysis, which was essentially the analysis method reported by Anderson and Glicksman[5] generalized to include d waves. The accuracy of our absolute counter efficiency measurements was ± 5.5 %.

II. EXPERIMENTAL ARRANGEMENT

A. Magnet System and Pion Beams

Our experimental arrangement is shown in Fig. 1. Negative pions created on a beryllium target internal to the Berkeley 184-in. synchrocyclotron were momentum-analyzed and focused onto a liquid hydrogen target. The pion beam was collimated by a 1-3/4-in. diameter brass tube through a 2-ft-thick lead wall. Two quadrupole magnets were used in focusing the beam onto the hydrogen target and preserved beam intensity sufficiently to allow our using a small-diameter collimator. The intensity of the transmitted beam was 20×10^3 pions per sec (time-average rate).

Energies and muon contaminations of our pion beams were determined from range curves in copper. Table I summarizes the pion beam characteristics. The mean energies at the center of the liquid hydrogen target includes a 1.5-Mev subtraction for loss of incident-pion energy in the first half of the hydrogen target.

The electron contamination in these beams was measured for the 230- and 290-Mev beams by using a gas Cherenkov counter[6] as the central unit in a three-counter telescope. This counter was unavailable during the run at 260, 317, and 371 Mev. Calculated electron contaminations agree well with the measurements.

Figure 2 shows horizontal and vertical pion beam profiles at the position of the hydrogen target. The profiles were measured by a 1-in.-diam counter in coincidence with the beam monitor counters. Profile width due to 1-in. counter resolution is subtracted from Fig. 2.

Table I. Characteristics of negative pion beams

Energy (Mev)	ΔT (Mev)	% Muons	% Electrons
230	± 8	10 ± 1.0	4.7 ± 1.0[a]
260	± 7	10 ± 1.0	3 ± 2[b]
290	± 9	7.4 ± 0.8	1.0 ± 0.5[a]
317	± 8	6.0 ± 1.0	2 ± 1[b]
371	± 9	4.0 ± 1.0	2 ± 1[b]

[a] Electron contamination measured with gas Cherenkov counter.

[b] Electron contamination estimated by calculation.

cycle. At least three cycles were completed for each incident pion energy. No net counting rate was found statistically at variance with those of different cycles. Table II shows typical counting rates for 260-Mev incident negative pions.

We took special precautions at 0 and 10 deg. At 0 deg the incident pion beam traversed the counter and was electronically rejected by the anti-coincidence counter. We made careful jamming checks for various incident pion fluxes. Forward data were found independent of beam flux below 8000 incident pions per sec on a time-average basis. Fluxes from 13,000 to 17,000 incident pions per sec (time average) were used for angles of 20 deg or greater.

ANALYSIS

Most reported experiments analyze the observed gamma-ray angular distributions by using

$$\frac{d\sigma_\gamma}{d\omega} = \frac{(\gamma/M)_{net}}{ntfG\Delta\Omega\bar{\epsilon}} , \tag{3}$$

where $(\gamma/M)_{net}$ is the net gamma-ray counting rate per incident pion, nt is the target thickness in protons/cm^2, f is the pion percentage of the beam, $G\Delta\Omega$ is the corrected solid angle is sr, and $\bar{\epsilon}$ is the detector efficiency for the average gamma-ray energy observed at a given angle. The gamma-ray differential cross section is fitted to the function

$$\frac{d\sigma_\gamma}{d\omega} = \sum_\ell b_\ell P_{\ell-1}(\alpha). \tag{4}$$

(We chose to designate the coefficients as a_1 through a_5 so that ℓ corresponds to the order of the fit. For this reason we express the differential cross section in the form above rather than have ℓ correspond to the order of the Legendre polynomial.

The charge-exchange differential cross section is then obtained in the form

$$\frac{d\sigma_{\pi^0}}{d\omega} = \sum_{\ell} a_{\ell} P_{\ell-1}(\alpha) \tag{5}$$

by use of the fact that each a_ℓ is directly proportional to the corresponding b_ℓ.[8]

This treatment is not quite correct, however. The detector efficiency for the gamma ray of the average energy used in Eq. (3) is not a good approximation to the average detection efficiency at a given angle, since we know the incident gamma rays range widely in energy and the detector efficiency varies rapidly with energy. The above makes clear the need for a more exact method of analysis.

The analysis method,[5] generalized to include d-wave scattering, is outlined below with a brief explanation of our least-squares analyses.

Beginning with Eq. (5), expressing the charge-exchange cross section in terms of the desired coefficients, a_ℓ, one derives the gamma-ray differential cross section in the laboratory frame,

$$\frac{d\sigma_\gamma}{d\Omega} = \frac{1}{(\gamma_0 - n_0 z)^2} \sum_{\ell=1}^{5} a_\ell P_{\ell-1}(y) \int_{-1}^{+1} \frac{P_{\ell-1}(x)dx}{(\gamma - nx)^2} \quad . \tag{6}$$

Figure 6 and Table III define the nomenclature. The integral of Eq. (6) expresses the analytical form for the gamma-ray spectrum observed at a given angle. The gamma-ray differential cross section is related to the observed counting rates by defining an "apparent" cross section for gamma-ray production in the center-of-mass system,[5]

$$\frac{d\sigma_\gamma}{d\Omega} = \frac{(\gamma/M)_{net}\,(\gamma_\theta - n_\theta z)^2}{ntfG\Delta\Omega} \quad . \tag{7}$$

Equating (6) and (7), we have

$$\frac{(\gamma/M_{net}\,(\gamma_0 - n_0 z)^2}{ntfG\Delta\Omega} = \sum_{\ell=1}^{5} a_\ell P_{\ell-1}(y) \int_{-1}^{+1} \frac{\epsilon(x,z)\,P_{\ell-1}(x)dx}{(\gamma-nx)^2} \quad , \tag{8}$$

where the explicit detector efficiency $\epsilon(x,z)$ has been placed under the integral sign. The quantity $G\Delta\Omega$ depends slightly on x and should ideally be included in the integrand of (8). Neglecting this dependence formally is a very good approximation because the dependence is slight and suitable averages have been made for the quantity $G\Delta\Omega$.

The analysis treatment is exact except for this approximation.

To express (8) in convenient form for least-squares solution for the coefficients, a_ℓ, we define

$$Y(z) = \frac{(\gamma/M)_{net}\,(\gamma_0 - n_0 z)^2}{ntfG\Delta\Omega} \quad , \tag{9}$$

$$\overline{\epsilon_\ell(z)} = \frac{1}{K_\ell} \int_{-1}^{+1} \frac{\epsilon(x,z)P_{\ell-1}(x)}{(\gamma-nx)^2}\,dx, \tag{10}$$

$$K_\ell = \int_{-1}^{+1} \frac{P_{\ell-1}(x)}{(\gamma-nx)^2}\,dx. \tag{11}$$

Finally we obtain a set of linear equations

$$Y(z) = \sum_{\ell=1}^{5} a_\ell X_\ell(z), \tag{12}$$

where

$$X_\ell(z) = P_{\ell-1}(y)\bar{\epsilon}_\ell(z) K_\ell \tag{13}$$

and

$$y = \left(\frac{\gamma_0 z - n_0}{\gamma_0 - n_0 z}\right). \tag{14}$$

There are as many equations in the set (12) as there are laboratory-system observing angles.

The integrals $\bar{\epsilon}_\ell(z)$ and K_ℓ are integrable in closed form. Numerical evaluation of the expressions for $\bar{\epsilon}_\ell(z)$, K_ℓ, $P_{\ell-1}(y)$, and $X_\ell(z)$ was performed by using the IBM 650 computer.

We now define the least-squares problem and outline its solution. The least-squares problem is to solve sets of Eqs. (12) for the coefficients a_ℓ. We have either nine or ten such equations in each set. A special characteristic of our problem is that the quantities $X_\ell(z)$ are not members of a complete orthonormal set of functions. We applied the general least-squares theory of Deming[9] to our problem and programmed it for IBM 650 computation.

This program performs a least-squares solution of (12) for coefficients a_ℓ, considering as many as 10 variables $Y(z)$, 50 variables $X_\ell(z)$ and 5 parameters a_ℓ. Fewer variables and coefficients may be used at the programmer's discretion. The variables $X_\ell(z)$ need not have any particular functional properties. The program first obtains a trial solution for the coefficients, a_ℓ, by solving five or fewer of the equations (12) by a matrix-inversion subroutine. The program then uses the trial solution to obtain final values for the a_ℓ by minimizing the least-squares sum of weighted residuals. In practice we found, as expected,[9] two or more iterations do not improve the solution.

Input data required for program are the experimental values of $Y(z)$, $X_\ell(z)$, their weights defined by

$$W_{Y(z)} = \frac{1}{(\Delta Y(z))^2} , \tag{15}$$

$$W_{X_\ell(z)} = \frac{1}{(\Delta X_\ell(z))^2} , \tag{16}$$

the number of equations in the set, and the number of parameters, a_ℓ, to be used in the fit. The errors, $\Delta Y(z)$ and $\Delta X_\ell(z)$, were computed by propagating, through the expressions for $\Delta Y(z)$ and $\Delta x_\ell(z)$, the errors assigned to their individual factors.

RESULTS

We present the results in two parts: (A) results of the experimental observations, and (B) results of the least-squares analyses based on the observations.

A. Experimental Results

Figure 7 shows the observed gamma-ray angular distribution. Table III presents the angle-independent experimental results. Table IV presents the angle-dependent experimental results.

B. Analysis Results

The analysis gives the coefficients, a_ℓ; their errors, δa_ℓ; and statistical criteria for the goodness of a given fit. To study the presence of d-wave scattering in the charge-exchange reaction the following five fits of our observations were made to Eq. (12) at each energy:

(a) an s-wave fit using one coefficient (a_1),

(b) an s- and p-wave fit using two coefficients (a_1 and a_2).

(c) an s- and p-wave fit using three coefficients (a_1, a_2, and a_3),

(d) and 3-, p-, and d-wave fit using four coefficients (a_1, a_2, a_3, and a_4),

(e) and s-, p-, and d-wave fit using five coefficients (a_1, a_2, a_3, a_4, and a_5).

Results are shown in Table V. The reported errors in the coefficients were computed from the error matrices (Table VI) by the relation

$$(\delta a_\ell)^2 = c_{\ell\ell}\sigma^2 \tag{17}$$

where $c_{\ell\ell}$ is a diagonal element of the error matrix and σ is the variance of a function of unit weight. We chose $\sigma = 1.0$ for all fits. This choice conservatively estimates the errors, since estimates of σ^2 by external consistency of the data ranged from $\sigma^2 = 0.7$ to $\sigma^2 = 0.9$.

To obtain information concerning the adequacy of the fits to our data we performed two related statistical goodness-of-fit tests. The first is the Pearson χ^2 test and the second is the so-called F test, which supplements the χ^2 test.[10, 11]

A χ^2 test obtains a criterion for the number of coefficients that must be included in the fitting function to adequately fit the data. The value of the least-squares sum of weighted residuals and the number of degrees of freedom define a probability P--the probability that the value of χ^2 should exceed the value obtained by assuming a given fitting function. P will in general reach a plateau value as ℓ, the number of coefficients used in the fitting function, is increased. P is generally rather insensitive to the number of coefficients once the plateau values have been reached. The number of coefficients needed for the "best" fit is the smallest ℓ value on the plateau.

The plateau value of P may be used to decide whether the "best" fit indicated by the plateau is indeed a good fit.

An F test gives the probability, on the basis of the available data, that a given a_ℓ equals 0.[10]

Table VII presents the results of the χ^2 and F tests. At each energy the Pearson χ^2 probability, P, does indeed reach a definite plateau at $\ell = 3$, i.e., a three-parameter fit is the "best" fit. The absolute values of P on the plateaus indicate that at each energy the "best" fit is a good fit. The values of χ^2 are less than their expectation value, the number of degrees of freedom at each energy. This indicates that the experimental errors on the coefficients have been reported conservatively.[10] There is, as expected, a less than 1% probability at each energy that less than a three-coefficient fit is adequate. The results for the one- and two-coefficient fits are included to show the plateaus. We also note the relatively in sensitive behavior of the χ^2 probability for $\ell \geq 3$. If there were an increase in the importance of d-wave scattering with increasing energy one might expect to see a trend towards higher values of P for $\ell = 4$ and $\ell = 5$ fits relative to the P values for $\ell = 3$ fits. Table VII shows no such trend in the P values except at the lowest energy, 230 Mev, where there is little evidence for d-wave scattering in any π-p reaction. Finally, we observed that at each energy the F-test probability P indicates:

(a) a less than 0.1% probability for coefficient $a_3 = 0$, and

(b) reasonable probabilities for coefficients $a_4 = a_5 = 0$.

Figure 8 shows the coefficients a_ℓ as a function of incident pion kinetic energy. The results of Korenchenko and Zinov for a_1, and a_2, and a_3 are also shown.[3,4]

The charge-exchange total cross sections were computed by integrating Eq. (5):

$$\sigma = 4\pi (a_1 \pm \delta a_1) \tag{18}$$

Energy	Total Cross Section
230 Mev	30.4 ± 1.3 mb
260	25.4 ± 1.0
290	18.2 ± 0.8
317	17.6 ± 0.8
371	13.6 ± 0.6

COUNTER-TELESCOPE CALIBRATION

In a separate series of experiments the absolute efficiency of the counter telescope as a function of incident photon energy was measured directly from the response of the counter telescope to the bremsstrahlung beam of the Berkeley electron synchrotron.

Absolute measurements of the counter's response to bremsstrahlung of various peak energies and the counter's energy threshold together with knowledge of the bremsstrahlung spectra[12] allow one to directly evaluate the counter's efficiency.

The counter efficiency as an explicit function of incident photon energy, k, is given by

$$\epsilon(k) = a \ln \left(\frac{k}{k_{th}}\right), \tag{19}$$

where a is the parameter to be determined and k_{th} is the measured energy threshold of the counter, in Mev. The parameter a can be related to the measurements. The experimental results are $a = 0.136 \pm 0.007$ and $k_{th} = 13.5 \pm 0.50$ Mev.

We also measured the relative counter efficiency as a function of incident beam's position and angle of incidence upon the gamma-ray counter telescope (see Fig. 9).

CORRECTIONS

This section classifies the corrections into two groups: (A) those applied to the observed counting rates, and (b) those applied to the experimental geometry. Correction for pion beam contamination has been discussed in Section II.

A. Counting-Rate Corrections

This experiment had two possible sources of accidental gamma-ray counts: (a) random-noise accidentals due to high singles rates in the various coincidence channels, and (b) "beam bunching" accidentals due to more than one incident pion per cyclotron beam fine-structure bunch. Random-noise accidentals were shown by calculation to be negligible. The calculations were based on measured singles rates in each coincidence channel, coincidence resolving times, and beam duty factors. The "beam bunching" type of accidental arises from the monitor coincidence circuit's inability to resolve two incident pions within less than 1×10^{-8} sec, i.e., more than one incident pion per fine-structure bunch. Since each incident pion may produce an observed gamma-ray and only one incident pion is detected, accidental counts arise. These accidental counting rates were measured by delaying the monitor coincidence by one fine-structure interval, 5.4×10^{-8} sec, relative to the gamma-ray counter.

We corrected for gamma-ray counts lost owing to (a) photon attenuation in the aluminum vacuum jacket surrounding the liquid hydrogen container and (b) the Dalitz process,

$$\pi^0 \rightarrow \gamma + e^+ + e^- , \tag{20}$$

by which 0.73% of the gamma rays are replaced by an electron pair.[13] Photon attenuation was computed in consideration of the photon spectrum observed at each laboratory-system angle. We found that an average attenuation valid for all energies and all angles is 0.70% ± 0.30%. The total gamma-

ray loss due to both processes is estimated as 1.4%± 0.5%.

The radiative capture process,

$$\pi^- + p \rightarrow n + \gamma, \tag{21}$$

makes a small contribution to the observed counting rates. Knowing the negative-to-positive pion photoproduction ratio from deuterium,[14] and the differential cross section for positive pion photoproduction from hydrogen,[15, 16] we estimated the radiative capture cross section in the c.m. frame by detailed balancing,

$$\left(\frac{d\sigma}{d\omega}\right)_{\pi^- + p \rightarrow \gamma + n} = 2\left(\frac{\pi^-}{\pi^+}(\theta)\right)\left(\frac{P_\gamma}{P_{\pi^+}}\right)^2 \left(\frac{d\sigma}{d\omega}\right)_{\gamma + p \rightarrow \pi^+ + n}, \tag{22}$$

where P_γ and P_{π^+} are the photon and pion momenta, respectively.
We used this cross section to estimate the corresponding laboratory-system counting rates.

The inelastic reactions

$$\pi^- + p \rightarrow n + \pi^0 + \pi^0,$$

$$\pi^- + p \rightarrow p + \pi^- + \pi^0 \tag{23}$$

also make a contribution of a few percent to the gamma-ray counting rate. We estimated this contribution by assuming (a) that the π^0 angular distribution is isotropic and (b) that the total cross section for each reaction is equal to that measured for

$$\pi^- + p \rightarrow n + \pi^- + \pi^+ \tag{24}$$

by Perkins et al.[17]

B. Geometrical Corrections

Geometrical corrections were made to the quantities $G\Delta\Omega$, and nt of Eq. (9).

The factor G accounts for variation of the differential cross section for gamma-ray production over the range of angles detected at a given counter setting. Perkins et al. have reported a detailed discussion of our computation method for G.[17] This factor was found negligibly different from unity for all observation angles.

The corrected solid angle, $\Delta\Omega$, is given by

$$\Delta\Omega = \frac{A}{d^2}(1 + \alpha), \tag{25}$$

where A is the Pb converter's effective area in cm^2, d is the distance from Pb converter to hydrogen target center in cm, and α is the first-order solid-angle correction factor. Both factors α and G were computed by using IBM 650 programs. The Pb converter effective area, A, is 14.5% less than the geometrical area. This correction accounts for the decrease in detector efficiency for photons incident upon the counter face off center and off normal.

The target thickness, nt, is corrected for (a) variable target thickness due to bowing of the walls of the liquid hydrogen vessel, and (b) the appreciable variation of beam intensity with beam radius as shown by the beam profile measurements. The average target thickness is

$$nt = n \frac{\iint \rho(r)\, t(r, \theta)\, r dr d\theta}{\iint \rho(r)\, r dr d\theta}, \tag{26}$$

where $\rho(r)$ is the beam profile in relative units, $t(r, \theta)$ is the hydrogen vessel thickness in cm, and n is the liquid hydrogen density in protons/cm^3. The integrals of Eq. (26) were evaluated by a summation approximation made by dividing the beam profile into concentric rings about the beam axis and the circumference of each ring into quadrants,

$$\int\int \rho(r) r dr d\theta \approx \pi \sum_i \rho(r)\,(r_i^2 - r_{i-1}^2), \tag{27}$$

$$\int\int \rho(r) t(r,\theta) r dr d\theta \approx \frac{\pi}{4} \sum_i \sum_j \rho(r)(r_i^2 - r_{i-1}^2) t(r_i, \theta_j), \tag{28}$$

where the index i denotes the ith ring, the index j denotes the jth quadrant, $r = \frac{r_i + r_{i-1}}{2}$, and $t(r_i, \theta_j)$ is the average target thickness in the interval $\Delta r_i \Delta\theta_j$. The target thicknesses (in cm) were measured by micrometer by using the grid of dots on the hydrogen vessel walls. The average target thickness is $(4.59 \pm 0.09) \times 10^{23}$ protons/cm^2 This number is valid for the hydrogen vessel at liquid hydrogen temperature and includes a 1% correction for the residual hydrogen gas present during target-empty measurements.

CONCLUSION

We conclude on the basis of the statistical tests that only s and p waves are necessary to adequately fit our measurements from 230 to 371 Mev.

There appears to be no need to include d-wave scattering to fit charge-exchange experiments through 371 Mev. The published results below 220 Mev,[5, 8, 18-25] the results of Ashkin et al. at 220 Mev,[26] the results of Korenchenko and Zinov from 240 to 333 Mev,[3, 4] and the results of this experiment establish this statement.

The π^--p elastic scattering and π^+-p scattering measurements in our energy range appear to require d-wave scattering for adequate interpretation. A very brief summary of the results of these experiments is:

1. Goodwin et al. require d waves for the π^--p elastic scattering at 290, 371, and 427 Mev but not at 230 Mev;[2, 27]

2. Korenchenko and Zinov, for the π^--p elastic scattering reaction, show in their analyses at 307 and 333 Mev a slight preference for a d-wave fit, but their result is not conclusive;[3]
3. Foote et al. showed in the analysis of their recent π^+-p scattering experiment at 310 Mev, which included measurement of the recoil proton polarization, that d waves were necessary for obtaining an adequate fit to the data.[1]

These results raise the interesting question, Why are d waves not found necessary to fit adequately all three π-p reactions at 300 Mev and above? It is possible that the effect of the d-wave phase shifts for charge-exchange scattering just cancels out, or that the effects of inelastic π^0-meson-producing reactions cancels the d-wave contribution. Another possibility is that a significant relative error exists among the various experiments. The latter possibility seems rather unlikely, particularly when one compares the work of Goodwin and this experiment, which were performed simultaneously at 230 and 290 Mev. The 371-Mev measurements of both experiments were not simultaneous but were performed by using identical pion beams, the same hydrogen target and the same auxiliary equipment, and operating techniques standardized within our research group. Both the π^--p elastic scattering and π^--p charge-exchange total cross sections and angular distribution coefficients agree well with independent measurements of their respective reactions. Goodwin, et al.[2] and the authors have standardized the methods of interpreting the statistical goodness-of-fit criteria. These factors taken together tend to argue aganist significant relative errors between various experiments.

ACKNOWLEDGMENTS

We wish to express our appreciation to Professor A. Carl Helmholz and Professor Burton J. Moyer for their continuing interest in this research. We are also indebted to Mr. Howard S. Goldberg for invaluable assistance with the data reduction and IBM 650 programming; to Dr. Lester K. Goodwin for his extensive assistance during the experimental measurements; and to Mr. Duane D. Newhart, whose efforts resulted in a perfectly functioning liquid hydrogen target.

To Mr. James Vale, the cyclotron crew, Mr. Rudin Johnson, and the synchrotron crew, we extend thanks for their cooperation and efficient assistance during the experimental measurements.

References

1. Foote, Chamberlain, Rogers, Steiner, Wiegand, and Ypsilantis, Phase Shifts in π^+-p Scattering at 310 Mev, Lawrence Radiation Laboratory Report UCRL-8981, Nov. 1959.
2. Lester K. Goodwin, Robert W. Kenney, and Victor Perez-Mendez, Phys. Rev. Letters 3, 522 (1959).
3. S. M. Korenchenko and V. G. Zinov, International Conference on Mesons and Recently Discovered Particles, Padua-Venice, Sept. 1957.
4. V. G. Zinov and S. M. Korenchenko, Zhur. Eksptl. i Teoret. Fiz. 36, 618-619 (1959).
5. H. L. Anderson and M. Glicksman, Phys. Rev. 100, 268 (1955).
6. Victor Perez-Mendez and John H. Atkinson, Gas Cherenkov Counters, Lawrence Radiation Laboratory Report UCRL-8570, Dec. 1959.
7. Duane D. Newhart, Victor Perez-Mendez, and William L. Pope, Liquid-Hydrogen Target, Lawrence Radiation Laboratory Report UCRL-8857, Aug. 1959.
8. H. L. Anderson, E. Fermi, R. Martin, and D. E. Nagle, Phys. Rev. 91, 155 (1953).
9. W. E. Deming, Statistical Adjustment of Data (John Wiley and Sons, New York 1943), Chapters IV and VIII.
10. Peter Cziffra and Michael J. Moravscik, A Practical Guide to the Method of Least Squares, Lawrence Radiation Laboratory Report UCRL-8523, Oct. 1958.
11. R. D. Evans, The Atomic Nucleus (McGraw-Hill Book Co., New York 1955), Chapter 27.
12. L. I. Schiff, Phys. Rev. 83, 252 (1951). Calculations by Larry Higgins (UCRL) private communication.
13. P. Lindenfeld, A. Sachs, and J. Steinberger, Phys. Rev. 89, 531 (1953).

14. H. A. Bethe and F. de Hoffman, Mesons and Fields, Vol. II (Row-Peterson and Company, Evanston, Illinois 1955), Sec. 36.

15. G. Neugebauer, W. D. Wales, and R. L. Walker, Phys. Rev. Letters 2, 429 (1959).

16. F. P. Dixon and R. L. Walker, Phys. Rev. Letters 1, 458 (1958).

17. Walton A. Perkins, III, Positive-Pion Production by Negative Pions, Lawrence Radiation Laboratory Report UCRL-8778, June 1959.

18. J. Tinlot and A. Roberts, Phys. Rev. 95, 137 (1954).

19. D. Bodansky, A. M. Sachs, and J. Steinberger, Phys. Rev. 93, 1367 (1954).

20. E. Fermi, M. Glicksman, R. Martin, and D. Nagle, Phys. Rev. 92, 161 (1953).

21. Maurice Glicksman, Phys. Rev. 94, 1335 (1954).

22. Maurice Glicksman, Phys. Rev. 95, 1045 (1954).

23. J. Ashkin, J. P. Blaser, F. Feiner, and M. O. Stern, Phys. Rev. 105, 724 (1957).

24. E. Garwin, W. Kernan, C. O. Kim, and C. M. York, Phys. Rev. 115, 1295 (1959).

25. W. J. Kernan, C. M. York, and E. L. Garwin, Bull. Am. Phys. Soc. Ser. II, 4, 401 (1959).

26. J. Ashkin, J. P. Blaser, F. Feiner, and M. O. Stern, Phys. Rev. 101, 1149 (1956).

27. Lester K. Goodwin (Lawrence Radiation Laboratory), private communication.

Table II

Observed gamma-ray counts per million incident pions at 260 ± 7 Mev.

Target and converter condition	Type of Measurement	Angle (lab) (deg) 0	10	20	28.7	40	60	83.2	110	155.7
H_2 in	Real	173.25±1.46	137.54±1.88	96.44±1.01	75.79±1.20	51.80±0.71	25.79±0.54	11.94±0.33	9.51±0.27	11.12±0.34
Pb in	Accidental	9.17±0.97	2.50±0.79	3.40±0.58	2.86±0.52	2.80±0.53	1.47±0.38	0.88±0.33	0.43±0.25	0.72±0.16
H_2 in	Real	7.60±0.78	12.15±0.78	7.72±0.56	4.34±0.42	2.35±0.34	1.57±0.23	0.90±0.21	0.95±0.22	0.63±0.18
Pb out	Accidental	0.50±0.50	0.86±0.50	0.60±0.35	0.16±0.16	0.20±0.20	0.20±0.20	0.40±0.28	0	0
H_2 out	Real	83.13±1.47	55.08±1.77	17.20±0.65	7.76±0.34	6.06±0.42	3.00±0.31	1.88±0.22	1.80±0.18	2.60±0.22
Pb in	Accidental	7.75±1.40	2.15±0.57	1.14±0.40	0.83±0.21	1.00±0.38	0.60±0.35	0	0.45±0.20	0.86±0.20
H_2 out	Real	5.40±0.70	9.76±0.88	4.09±0.42	0.50±0.17	0.15±0.09	0	0.27±0.13	0.47±0.18	0.40±0.16
Pb out	Accidental	0	0.60±0.35	0	0	0	0	0.20±0.14	0.17±0.17	0
Net counting rates		87.00±2.92	79.98±3.07	73.95±1.95	62.32±1.44	41.95±1.13	20.55±0.86	8.76±0.66	7.08±0.56	8.43±0.54

Table III. Angle-independent experimental results used for the least-squares analyses

Energy (Mev)	$\bar{n}t$ (protons/cm^2)	f pion (%) in incident beam	γ	$\eta = \beta\gamma$	γ_0	$\eta_0 = \beta\gamma_0$
230	$(4.56 \pm 0.09) \times 10^{23}$	85.3 ± 1.4	2.138 ± 0.038	1.890 ± 0.044	1.036 ± 0.002	0.2711 ± 0.0062
260		87.0 ± 2.2	2.264 ± 0.029	2.031 ± 0.032	1.038 ± 0.001	0.2891 ± 0.0047
290		91.6 ± 1.3	2.385 ± 0.036	2.166 ± 0.039	1.047 ± 0.002	0.3111 ± 0.0058
317		92.0 ± 2.2	2.492 ± 0.031	2.283 ± 0.034	1.049 ± 0.002	0.3255 ± 0.0050
371		94.0 ± 1.5	2.699 ± 0.033	2.507 ± 0.036	1.060 ± 0.002	0.3578 ± 0.0050

Table IV. Angle-dependent experimental results used for the least-squares analyses

Angle (lab) (deg)	Net count rate: Raw data (corrected for accidentals only) (counts $\times 10^{-6}$)	Net count rate: Final corrected $(\gamma/M)_{net}$ (counts $\times 10^{-6}$)	$G \Delta \Omega$ (steradian)
230-Mev incident π^- mesons			
0	87.19 ± 2.45	88.24 ± 2.49	0.03700 ± .00037
10	78.20 ± 3.18	79.12 ± 3.21	0.03695 ± .00037
20	72.44 ± 1.21	73.28 ± 1.27	0.03673 ± .00037
30	61.17 ± 1.22	61.85 ± 1.26	0.03638 ± .00036
40	46.30 ± 0.96	46.77 ± 0.99	0.03599 ± .00036
60	22.94 ± 0.84	23.09 ± 0.85	0.03514 ± .00035
90	9.98 ± 0.55	9.97 ± 0.55	0.03458 ± .00035
120	11.04 ± 0.56	11.07 ± 0.56	0.03515 ± .00035
140	12.04 ± 0.53	12.09 ± 0.54	0.03599 ± .00036
155	13.92 ± 0.72	14.00 ± 0.73	0.03647 ± .00036
290-Mev incident π^- mesons			
0	86.26 ± 2.34	86.93 ± 2.49	0.03702 ± .00037
20	71.21 ± 1.35	71.69 ± 1.41	0.03673 ± .00037
30	52.77 ± 1.19	53.03 ± 1.24	0.03638 ± .00036
40	38.38 ± 1.06	38.49 ± 1.09	0.03599 ± .00036
60	14.47 ± 0.69	14.31 ± 0.70	0.03514 ± .00035
90	4.73 ± 0.50	4.55 ± 0.51	0.03458 ± .00035
120	4.53 ± 0.43	4.40 ± 0.43	0.03515 ± .00035
140	4.03 ± 0.37	3.91 ± 0.37	0.03599 ± .00036
150	5.00 ± 0.66	4.91 ± 0.66	0.03647 ± .00036
260-Mev incident π^- mesons			
0	87.00 ± 2.92	87.97 ± 2.95	0.03702 ± .00037
10	79.98 ± 3.07	80.87 ± 3.09	0.03695 ± .00037
20	73.95 ± 1.59	74.75 ± 1.64	0.03673 ± .00037
28.7	62.32 ± 1.44	62.97 ± 1.48	0.03644 ± .00036
40	41.95 ± 1.13	42.32 ± 1.15	0.03599 ± .00036
60	20.55 ± 0.86	20.65 ± 0.87	0.03514 ± .00035
83.2	8.76 ± 0.66	8.73 ± 0.66	0.03455 ± .00034
110	7.08 ± 0.56	7.05 ± 0.56	0.03480 ± .00035
155.7	8.43 ± 0.54	8.44 ± 0.54	0.03660 ± .00037
317-Mev incident π^- mesons			
0	84.31 ± 3.01	84.64 ± 3.06	0.03702 ± .00037
20	69.41 ± 1.31	69.58 ± 1.37	0.03673 ± .00037
28.7	58.42 ± 1.51	58.48 ± 1.57	0.03644 ± .00036
40.	40.14 ± 0.88	40.01 ± 0.95	0.03599 ± .00036
60	16.69 ± 0.63	16.39 ± 0.67	0.03514 ± .00035
83.2	5.08 ± 0.59	4.76 ± 0.62	0.03455 ± .00035
110	3.05 ± 0.44	2.80 ± 0.45	0.03480 ± .00035
140	4.06 ± 0.32	3.87 ± 0.34	0.03600 ± .00036
155.7	3.17 ± 0.42	3.00 ± 0.43	0.03660 ± .00037
371-Mev incident π^- mesons			
0	87.38 ± 2.86	86.10 ± 2.99	0.03702 ± .00037
10	75.23 ± 2.36	73.83 ± 2.49	0.03696 ± .00037
20	67.63 ± 1.47	66.24 ± 1.66	0.03673 ± .00037
28.7	54.91 ± 1.01	53.51 ± 1.20	0.03644 ± .00036
40	33.73 ± 0.73	32.38 ± 0.90	0.03599 ± .00036
60	14.03 ± 0.56	12.75 ± 0.69	0.03514 ± .00035
83.2	4.91 ± 0.43	3.92 ± 0.52	0.03455 ± .00035
110	2.65 ± 0.45	1.93 ± 0.50	0.03480 ± .00035
140	1.34 ± 0.35	0.72 ± 0.40	0.03600 ± .00036
155.7	2.90 ± 0.33	2.39 ± 0.39	0.03660 ± .00037

Table V. Results of the least-squares fits of the measurements to the function $\frac{d\sigma}{d\Omega} = \sum_{\ell} a_{\ell} P_{\ell-1}(\alpha)$ for different values of ℓ (the number of coefficients used for the fit) and k (the number of degrees of freedom). S is the least-squares sum of weighted residuals.

230 ± 8 Mev	$\ell = 1$, k = 8	$\ell = 2$, k = 7	$\ell = 3$, k = 6	$\ell = 4$, k = 5	$\ell = 5$, k = 4
a_1	3.24 ± .10	2.99 ± .10	2.50 ± .10	2.50 ± .10	2.50 ± .10
a_2	---	1.62 ± .16	1.39 ± .15	1.47 ± .16	1.47 ± .16
a_3	---	---	2.73 ± .28	2.77 ± .28	2.82 ± .30
a_4	---	---	---	0.29 ± .25	0.26 ± .26
a_5	---	---	---	---	-0.34 ± .78
S	183.7	85.35	2.41	1.09	0.89
260 ± 7 Mev	$\ell = 1$, k = 7	$\ell = 2$, k = 6	$\ell = 3$, k = 5	$\ell = 4$, k = 4	$\ell = 5$, k = 3
a_1	2.80 ± 0.08	2.20 ± 0.08	2.02 ± 0.08	2.02 ± 0.08	2.02 ± 0.08
a_2	---	2.18 ± 0.14	1.75 ± 0.14	1.76 ± 0.15	1.75 ± 0.15
a_3	---	---	2.15 ± 0.22	2.16 ± 0.22	2.20 ± 0.24
a_4	---	---	---	0.05 ± 0.19	0.03 ± 0.20
a_5	---	---	---	---	-0.25 ± 0.55
S	299.3	93.29	1.62	1.56	1.35
290 ± 9 Mev	$\ell = 1$, k = 7	$\ell = 2$, k = 6	$\ell = 3$, k = 5	$\ell = 4$, k = 4	$\ell = 5$, k = 3
a a_1	1.77 ± 0.06	1.68 ± 0.06	1.45 ± 0.06	1.45 ± 0.06	1.45 ± 0.06
a_2	---	1.81 ± 0.11	1.80 ± 0.10	1.77 ± 0.11	1.77 ± 0.11
a_3	---	---	1.89 ± 0.18	1.89 ± 0.18	1.91 ± 0.19
a_4	---	---	---	-0.17 ± 0.16	-0.18 ± 0.16
a_5	---	---	---	---	-0.16 ± 0.45
S	462.9	107.68	2.03	0.94	0.82
317 ± 8 Mev	$\ell = 1$, k = 7	$\ell = 2$, k = 6	$\ell = 3$, k = 5	$\ell = 4$, k = 4	$\ell = 5$, k = 3
a_1	1.51 ± 0.05	1.51 ± 0.06	1.40 ± 0.06	1.40 ± 0.06	1.39 ± 0.06
a_2	---	1.86 ± 0.10	1.85 ± 0.10	1.85 ± 0.10	1.87 ± 0.11
a_3	---	---	1.50 ± 0.17	1.49 ± 0.17	1.50 ± 0.17
a_4	---	---	---	0.02 ± 0.15	0.01 ± 0.15
a_5	---	---	---	---	-0.35 ± 0.42
S	514.2	82.44	1.69	1.65	0.93
371 ± 9 Mev	$\ell = 1$, k = 8	$\ell = 2$, k = 7	$\ell = 3$, k = 6	$\ell = 4$, k = 5	$\ell = 5$, k = 4
a_1	1.30 ± 0.04	1.18 ± 0.05	1.08 ± 0.05	1.08 ± 0.05	1.08 ± 0.05
a_2	---	1.72 ± 0.08	1.63 ± 0.08	1.62 ± 0.08	1.62 ± 0.08
a_3	---	---	1.18 ± 0.12	1.18 ± 0.12	1.16 ± 0.13
a_4	---	---	---	-0.07 ± 0.11	-0.06 ± 0.11
a_5	---	---	---	---	0.16 ± 0.27
S	660.5	94.23	4.47	4.12	3.80

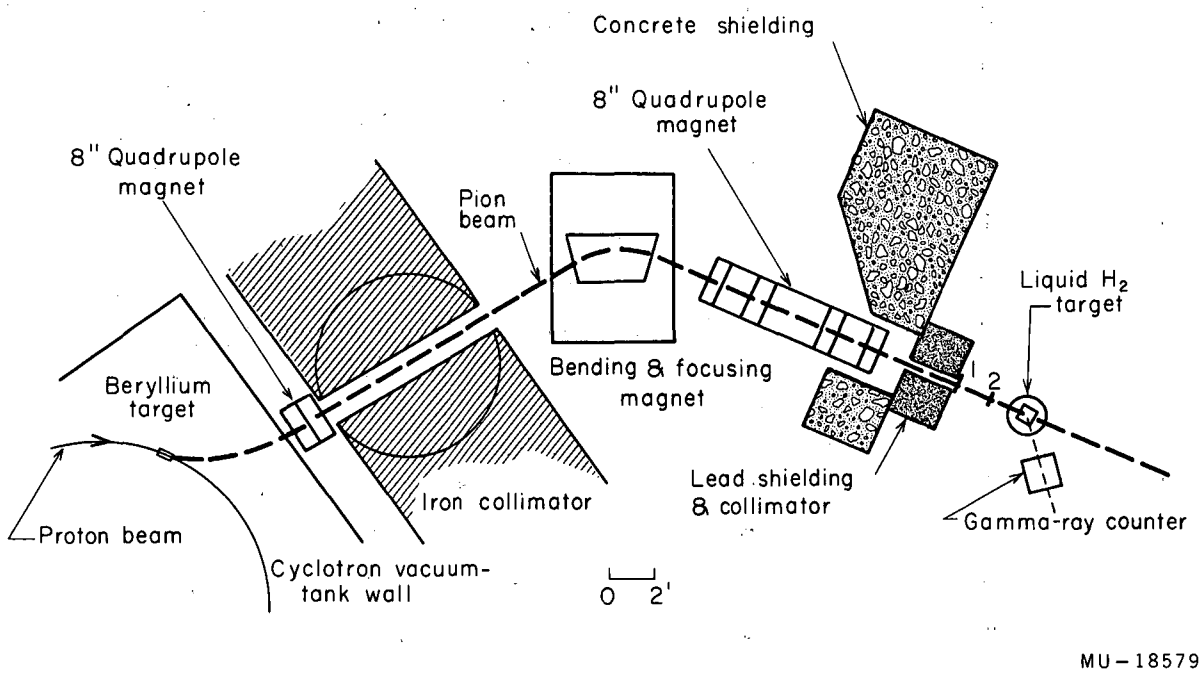

Fig. 1. Diagram of the experimental arrangement.

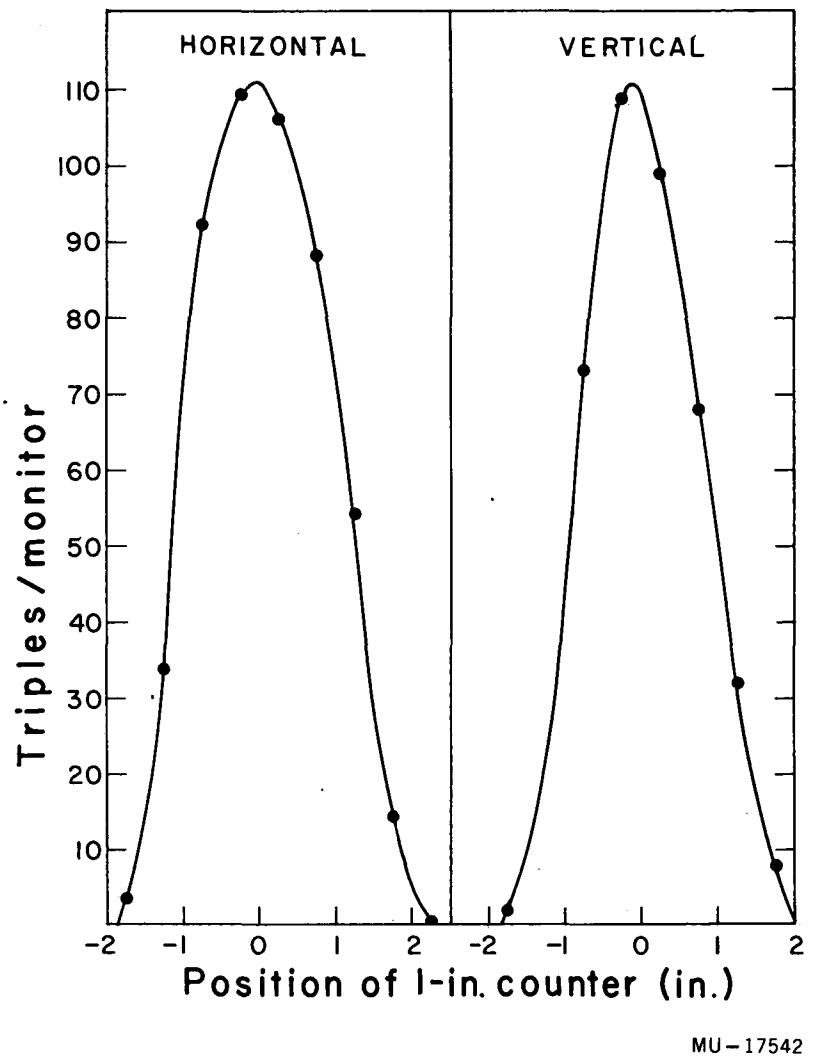

Fig. 2. Horizontal and vertical beam profiles measured at the position of the liquid hydrogen target.

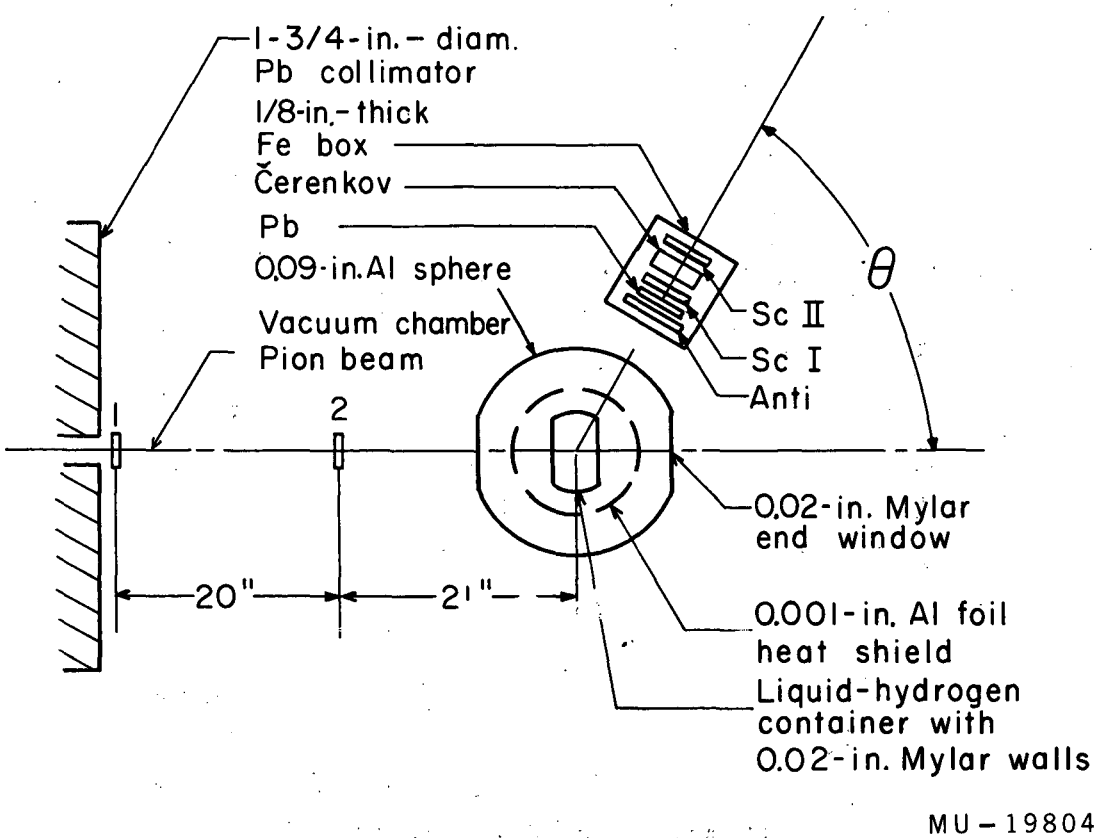

Fig. 3. Liquid hydrogen target and counter telescope.

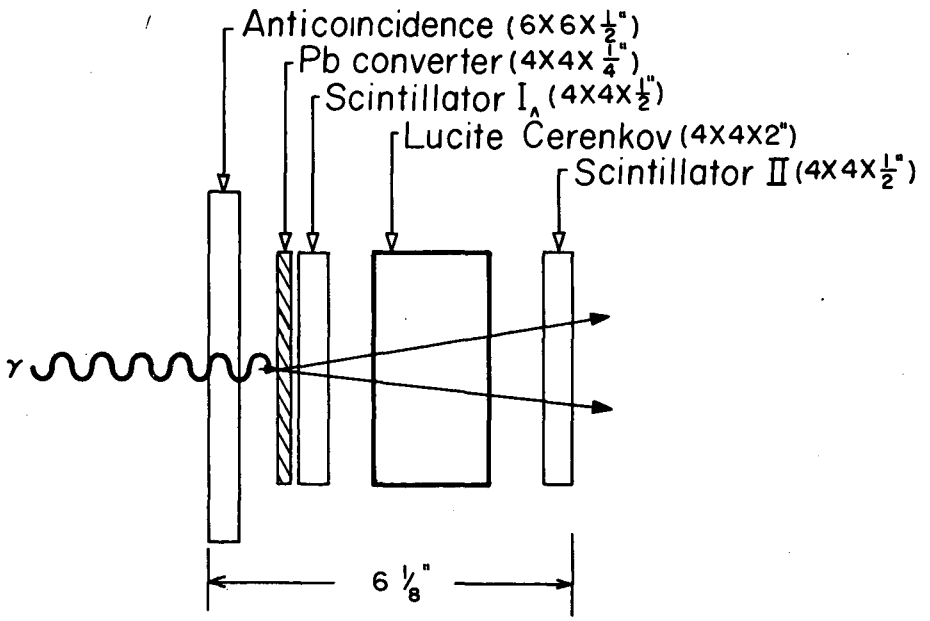

MU-18583

Fig. 4. Gamma-ray counter telescope schematic.

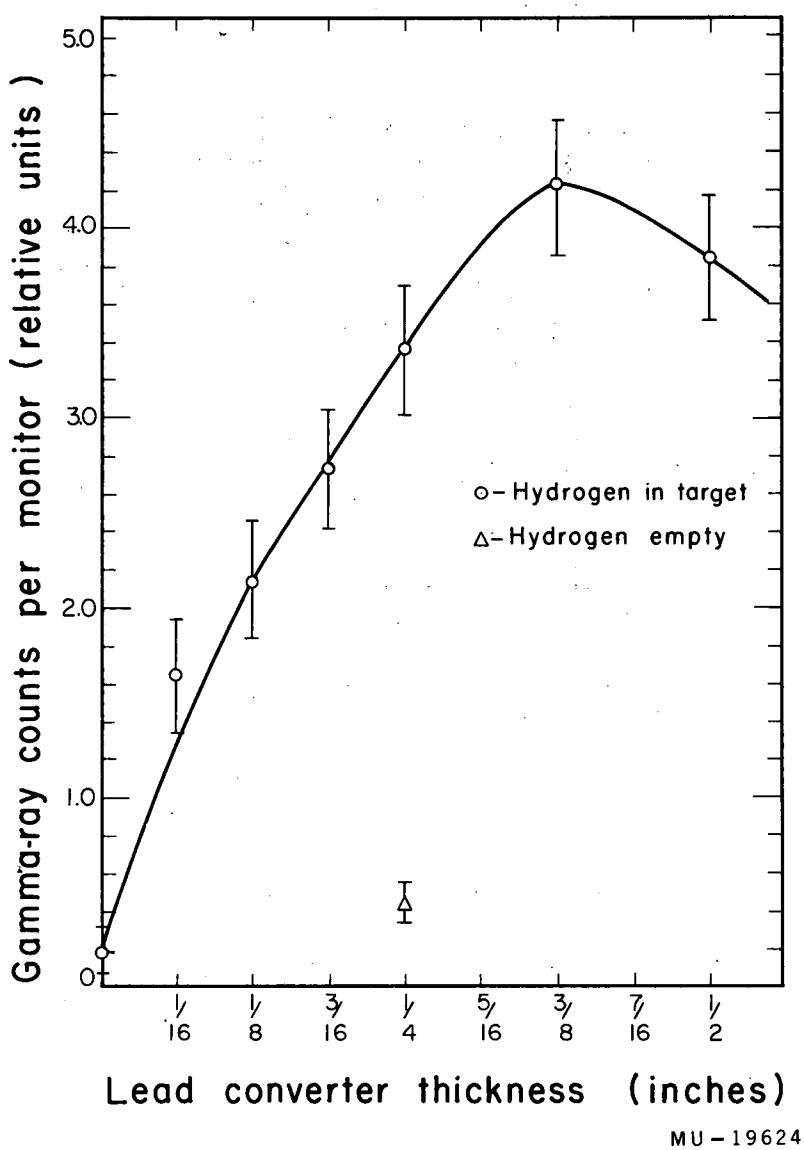

Fig. 5. Gamma-ray telescope counting rate as a function of Pb converter thickness. The lead-in to lead-out ratio is 17 to 1 for 1/4-in. lead converter. The target-full to target-empty ratio is 8 to 1 for a 1/4-in. lead converter. This curve was obtained at 40 deg (lab).

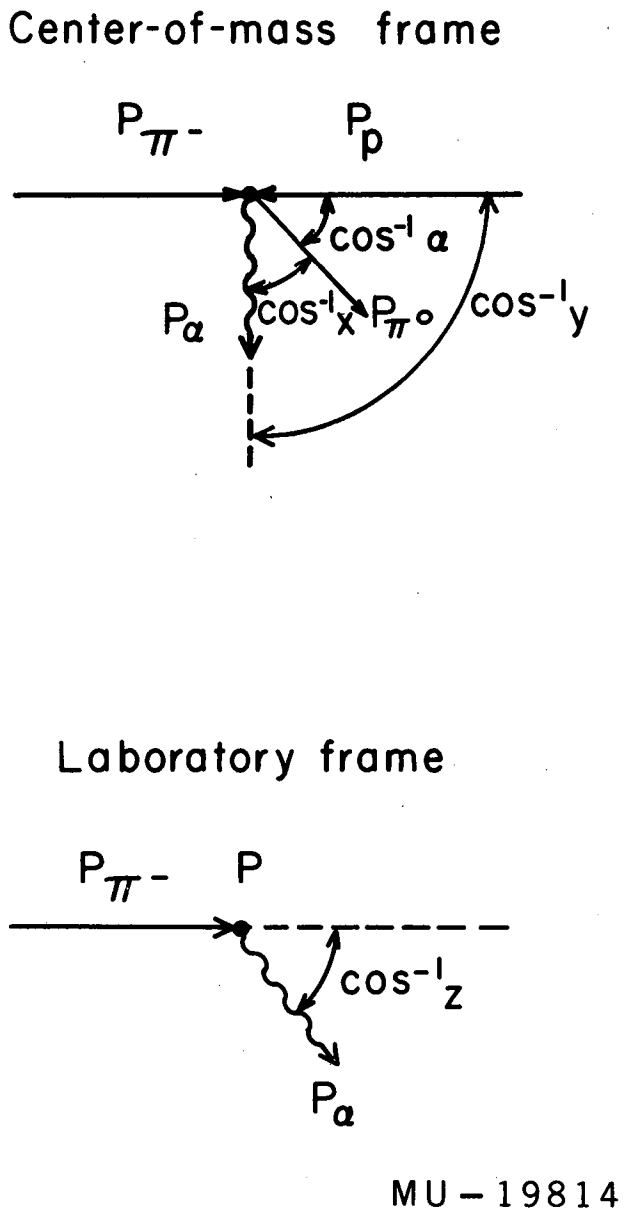

Fig. 6. Definitions of the angles involved in the derivation of the analysis method.

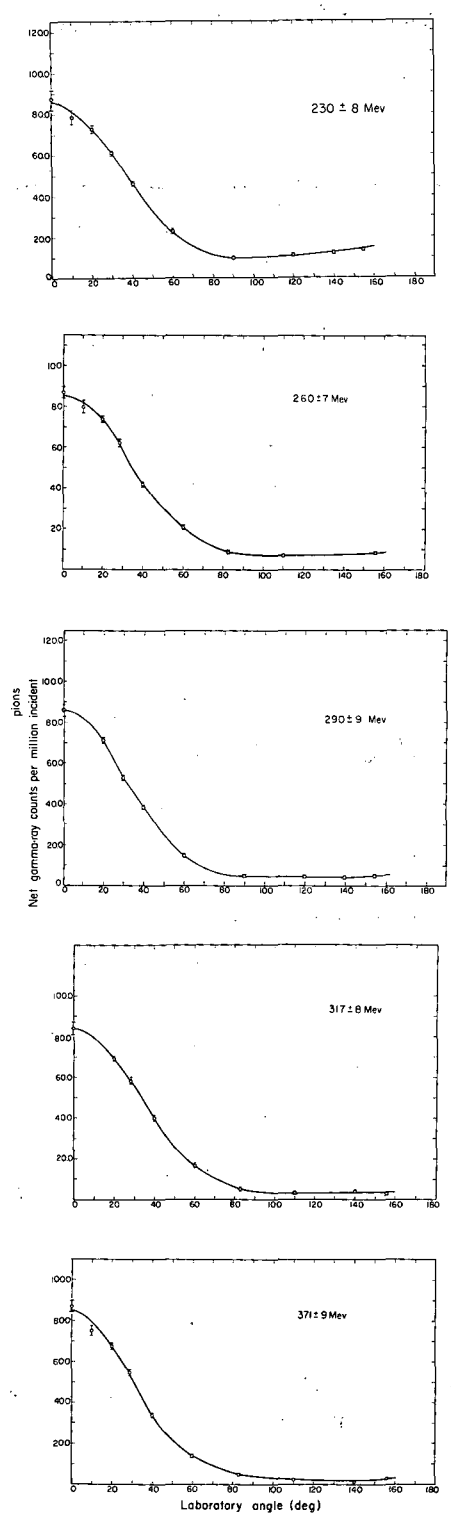

MUB-427

Fig. 7. Observed gamma-ray angular distributions.

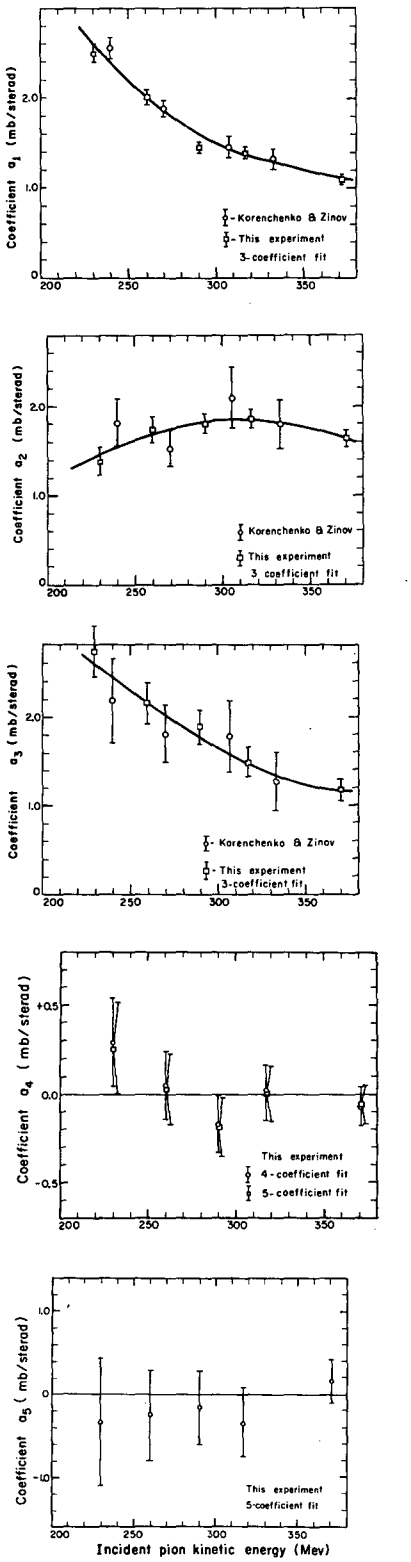

MUB-428

Fig. 8. Coefficients a_ℓ as a function of incident pion kinetic energy.

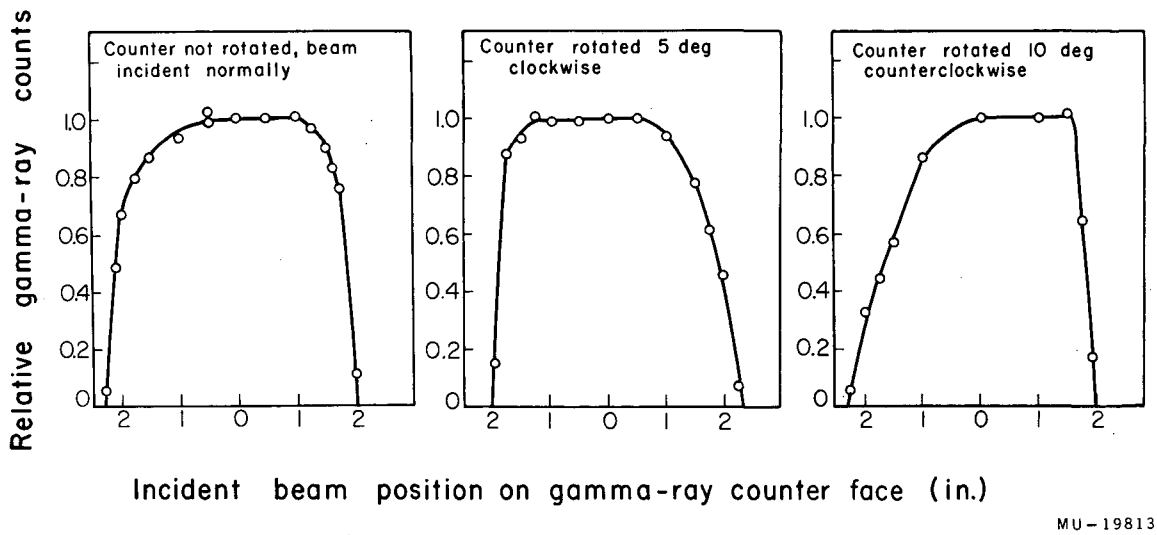

Fig. 9. Relative gamma-ray efficiency measurements as a function of incident beam position and incidence angle.

This report was prepared as an account of Government sponsored work. Neither the United States, nor the Commission, nor any person acting on behalf of the Commission:

A. Makes any warranty or representation, expressed or implied, with respect to the accuracy, completeness, or usefulness of the information contained in this report, or that the use of any information, apparatus, method, or process disclosed in this report may not infringe privately owned rights; or

B. Assumes any liabilities with respect to the use of, or for damages resulting from the use of any information, apparatus, method, or process disclosed in this report.

As used in the above, "person acting on behalf of the Commission" includes any employee or contractor of the Commission, or employee of such contractor, to the extent that such employee or contractor of the Commission, or employee of such contractor prepares, disseminates, or provides access to, any information pursuant to his employment or contract with the Commission, or his employment with such contractor.